Chapter 1

Introduction

This thesis is concerned with the transfer of energy from light to matter. Over a century ago it was established that light consists of packets of energy [1], now known as photons. Not much later the energy levels of matter at the atomic scale were found to be discrete [2]. These phenomena required a new physical description that has become the theory of quantum mechanics [3]. Now, this theory of light and matter could contribute to tackling a fundamental socioeconomic and technological challenge: To find a sustainable supply of useful energy that is cheap, abundant and generated on-the-spot.

For this purpose the sun is the most obvious energy source as it is abundant and readily available almost everywhere. Evolution has developed a mechanism to capture and convert solar irradiation and fixate atmospheric carbon, known as photosynthesis. Ironically, one of the major societal concerns today regarding the supply of energy is related to the re-emission of this carbon millions of years after it was sequestrated. Nevertheless, the bulk of the energy supply remains fossil, illustrating that the dependence on energy is deeply rooted. This is not surprising as the availability of affordable energy is highly correlated with living standards. It also tells that there is no current alternative. Therefore, a technology that can generate fuel or electricity from solar irradiation in real-time would be an elegant solution.

Mimicking the highly efficient sunlight to charge, and charge to fuel conversions in photosynthesis has become the objective of a scientific field called artificial photosynthesis [4,5]. In this work, the processes initiated by the absorption of a solar photon in photosynthetic complexes (**Chapters 3,4 and 6**) as well as biomimetic systems (**Chapters 5 and 7**) are analyzed. The mixing of quantum states through resonant coherent nuclear motion is found to drive the efficient conversion of light into separated charges in the first section (**Chapters 3-5**). In the final part (**Chapters 6-7**) results are presented on stabilizing separated charges and the interfacing with catalysis.

1.1 Artificial Photosynthesis

Generating fuel from sunlight and water is a conceptually simple process (Figure 1.1). An incident solar photon is absorbed by a molecule resulting in an excited state ($molecule \rightarrow molecule^*$). The neutral excited electron-hole pair (exciton) undergoes charge separation through the transfer of an electron to a mediator, while the electron vacancy (the hole) is transferred to a different mediator.

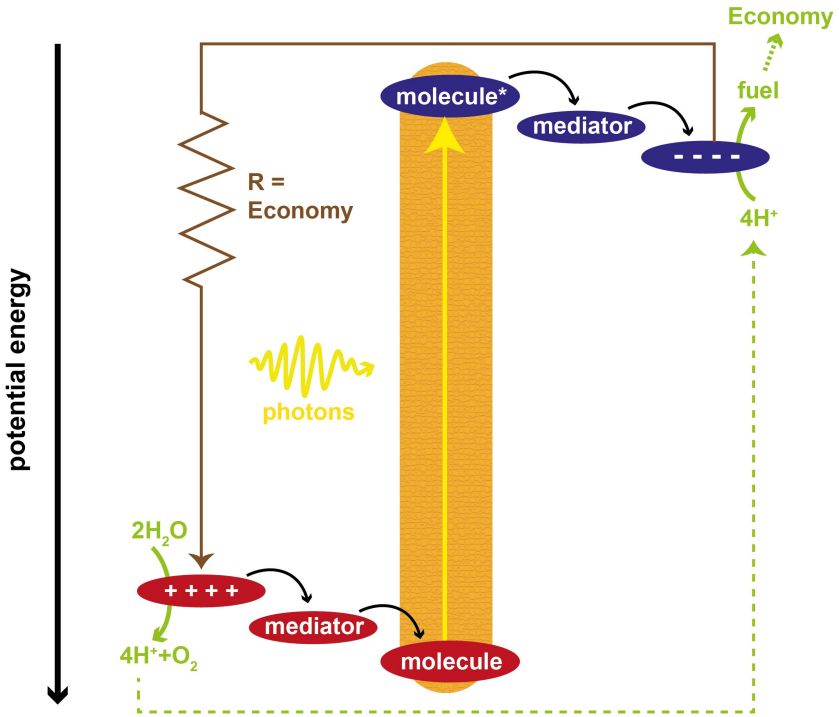

Figure 1.1: Supplying the economy with energy from the sun can be either achieved through photoproduction of electricity (brown) or fuel (green).

Mediators are required to spatially separate the electron and hole. The movement of a hole is also an electronic process. In the conventional picture it is transferred by means of an electron from a neighbouring molecule filling the positive vacancy, thereby displacing the hole from its initial site to the new molecule. The transfer of charge from an excited state of a molecule to a mediator is a quantum mechanical process that involves the system changing its quantum mechanical state.

Metal oxides are known to be good mediators for photoexcited electrons [6]. The early 90's also saw the development of polymer systems that rapidly transfer the photoexcited electrons to buckminsterfullerene (C60) [7]. Both systems, now referred to as dye-sensitized and bulk-heterojunction solar cells, are becoming commercially available for small-scale electricity generation [8]. A promising hole mediator is the recent molecule found by Moore and coworkers [9] that mimics an ingenious mechanism in oxygenic photosynthesis to store positive charges (see **Chapter 7**). The most efficient systems for direct photoinduced water splitting (e.g. [10]) unfortunately still contain very expensive semiconducting components.

In this context, the screening of large numbers of molecules for their potential to produce stable charge separated states is crucial to find more efficient systems for artificial photosynthesis. As it is far from trivial to synthesize molecules, smart strategies are needed to answer questions such as:

(1) What is the fraction of solar irradiation that is absorbed by the molecules?

(2) What is the percentage of absorbed photons that actually evolve into stable charge separated states?

Quantum Mechanics (QM) contains the answers to these questions. In the following QM will be introduced in the context of solar energy transduction within Schrödinger's picture of QM as this most closely resembles the computational methods employed in this thesis. In section 1.1.3 the concepts of coupling and coherence will briefly be discussed. Atomic units are used throughout.

1.1.1 Solar Light Absorption

The first step in considering question **(1)** - from a computational chemists perspective - is to find the ground state energy E_0 from Schrödinger's time-independent equation:

$$\hat{\mathcal{H}}(\boldsymbol{r}, \boldsymbol{R}(t))\Psi_0(\boldsymbol{r}, \boldsymbol{R}(t)) = E_0(\boldsymbol{R}(t))\Psi_0(\boldsymbol{r}, \boldsymbol{R}(t)), \tag{1.1}$$

where $\Psi_0(\boldsymbol{r}, \boldsymbol{R}(t))$ is the ground state wavefunction that is a function of the coordinates of the electrons $\boldsymbol{r}$ and nuclei $\boldsymbol{R}(t)$. The time-dependence $\boldsymbol{R} = \boldsymbol{R}(t)$ is added explicitly to emphasize that the wavefunction *does* change as the nuclear positions evolve in time. $\hat{\mathcal{H}}(\boldsymbol{r}, \boldsymbol{R}(t))$ is the total unperturbed time-independent Hamiltonian. The total set of eigenvalues

including excited states can be found by considering the full spectrum of the Hamiltonian[1]:

$$\hat{\mathcal{H}}(\boldsymbol{r}, \boldsymbol{R}(t)) \begin{pmatrix} \Psi_0 \\ \Psi_1 \\ \Psi_2 \\ \vdots \\ \Psi_i \end{pmatrix} = \begin{pmatrix} E_0 & 0 & 0 & \cdots & 0 \\ 0 & E_1 & 0 & \cdots & 0 \\ 0 & 0 & E_2 & \cdots & 0 \\ \vdots & \vdots & \vdots & \ddots & \vdots \\ 0 & 0 & 0 & \cdots & E_i \end{pmatrix} \begin{pmatrix} \Psi_0 \\ \Psi_1 \\ \Psi_2 \\ \vdots \\ \Psi_i \end{pmatrix}. \tag{1.2}$$

For every transition between the ground state and an excited state i an oscillator strength f_i can be calculated [11]:

$$f_i = {}^2/_3(E_i - E_0)|\langle\Psi_0|\hat{\mu}|\Psi_i\rangle|^2, \tag{1.3}$$

where the energy gap $(E_i - E_0)$ is the excitation or photon energy (ε_i) required to bring the system from the ground state to excited state i and $\hat{\mu}$ is the dipole moment operator. In Figure 1.2 the oscillator strengths of a hypothetical molecule are plotted with the solar irradiation spectrum.

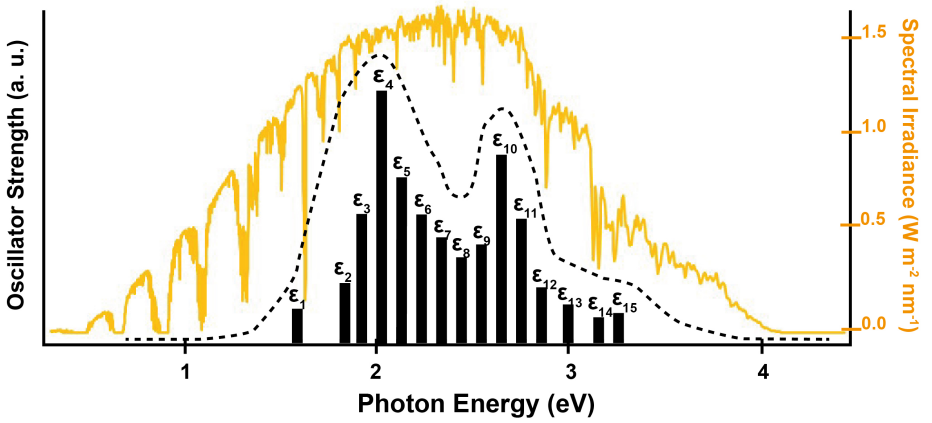

Figure 1.2: Comparison of the solar irradiation spectrum (AM 1.5, orange line) with a schematic representation of the excitation energies ε_i and their respective oscillator strength.

Calculating the overlap between the convoluted excitations (dotted line, figure 2.1) obtained from QM and the solar spectrum provides a reasonable answer to question **(1)**.

[1] Note that *electron-nuclear* wavefunctions are discussed (not molecular orbitals), therefore the lowest eigenfunction is the ground state $\Psi_0(\boldsymbol{r}, \boldsymbol{R}(t))$.

1.1.2 Photoinduced Charge Separation

The more difficult question is **(2)**. The static QM picture discussed so far doesn't provide the necessary information to successfully answer **(2)**. To simulate whether the excited states $\Psi_i(\boldsymbol{r}, \boldsymbol{R}(t))$ will undergo charge separation - again from a computational chemists perspective - requires solving the time-dependent Schrödinger equation:

$$i\frac{\partial\Psi(\boldsymbol{r}, \boldsymbol{R}, t)}{\partial t} = \hat{\mathcal{H}}(\boldsymbol{r}, \boldsymbol{R}(t))\Psi(\boldsymbol{r}, \boldsymbol{R}, t). \tag{1.4}$$

This can be achieved by constructing the time-dependent wavefunction $\Psi(\boldsymbol{r}, \boldsymbol{R}, t)$ from a basis of time-independent wavefunctions that are eigenstates of the Hamiltonian [12]:

$$\Psi(\boldsymbol{r}, \boldsymbol{R}, t) = \sum_i c_j(t)\Psi_j(\boldsymbol{r}, \boldsymbol{R}(t)). \tag{1.5}$$

where $c_j(t)$ are the time-dependent coefficients that can be seen as the weights of the specific states in the total wavefunction. The stationary eigenstates change as the nuclear coordinates $R(t)$ evolve in time. Therefore, different excited states can be prepared through the initial conditions of the time dependent coefficients:

$$c_1(0) = 0, \cdots, c_i(0) = 1, \cdots, c_j(0) = 0, \tag{1.6}$$

where these initial conditions correspond to the molecule in excited state i after absorption of a photon with energy $(E_i - E_0)$. To properly answer **(2)** one would need to prepare initial conditions 1.6 for all excited states with non-negligible oscillator strength, substitute the resulting expansions 1.5 into equation 1.4 and evolve $\Psi(\boldsymbol{r}, \boldsymbol{R}, t)$ starting from a statistically representative ensemble of nuclear coordinates for each excited state.

A way to interpret the results is the visualization of the excited state progression through the spatial difference in particle density between spin up and spin down electrons (this is done within Kohn-Sham in **Chapter 5**)[2]:

$$\begin{aligned} PSD(\boldsymbol{r}, t) = N \int \Psi^*([\boldsymbol{r}, \uparrow]\boldsymbol{x}_2 \cdots \boldsymbol{x}_N)\Psi([\boldsymbol{r}, \uparrow]\boldsymbol{x}_2 \cdots \boldsymbol{x}_N)\mathrm{d}\boldsymbol{x}_2 \cdots \mathrm{d}\boldsymbol{x}_N \\ -N \int \Psi^*([\boldsymbol{r}, \downarrow]\boldsymbol{x}_2 \cdots \boldsymbol{x}_N))\Psi([\boldsymbol{r}, \downarrow]\boldsymbol{x}_2 \cdots \boldsymbol{x}_N)\mathrm{d}\boldsymbol{x}_2 \cdots \mathrm{d}\boldsymbol{x}_N, \end{aligned} \tag{1.7}$$

[2]This visualization method will not give the charge transfer when spin and charge decouple (as observed in Chapter 7).

where N is the total number of electrons. If the excited electron is spin up, negative regions of the $PSD(\boldsymbol{x}, t)$ will represent the photoinduced hole, whereas the positive regions will represent the photoinduced electron. In most cases, excited states with significant oscillator strength are of excitonic character, meaning that the electron and hole regions of the $PSD(\boldsymbol{x}, t)$ overlap significantly as visualized in Figure 1.3 for a hypothetical linear molecule.

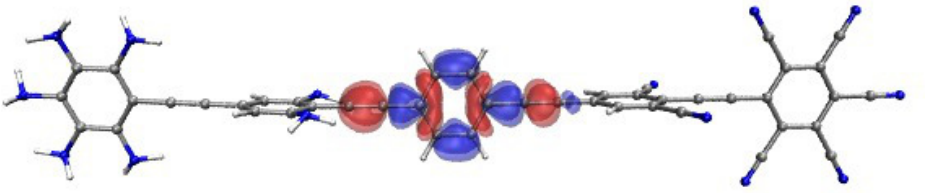

Figure 1.3: Spatial distribution of the $PSD(\boldsymbol{x}, 0)$ in a hypothetical linear molecule for an excitonic state. The red isosurface corresponds to the photoinduced hole and the blue isosurface to the photoinduced electron (*Isosurfaces are visualized through the Kohn-Sham equivalent of equation 1.8: see Chapter 5, equation 5.5*).

However, the $PSD(\boldsymbol{x}, 0)$ need not be symmetric as in Figure 1.3. The initial excited state in vision, for example, is significantly polarized [13]. Charge transfer states generally are characterized by a large(r) spatial separation between the hole and electron regions of the $PSD(\boldsymbol{x}, t)$ (Figure 1.4).

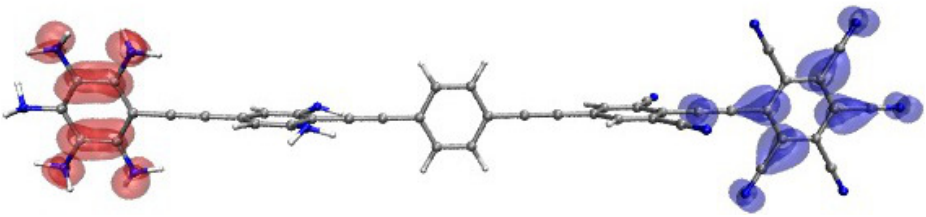

Figure 1.4: Spatial distribution of the $PSD(\boldsymbol{x}, \tau)$ in a hypothetical linear molecule for a charge transfer state.

With this interpretation scheme, all the different time traces can be visualized to follow the progression of the excited states. This will enable a quantitative assessment of the progression of initial excitonic states into lower lying charge transfer states and provide an answer to **(2)**.

1.2 Coupling and Coherence

In practice, the wavefunctions are not known and equation 1.4 and expansion 1.5 in section 1.1.2 need to be approximated (see **Chapter 2**). This is not trivial and requires significant computational resources even for short simulations of small molecules. Therefore, an understanding of the underlying physical or chemical process is important.

Consider substituting expansion 1.5 in equation 1.4 and projecting both sides of the resulting equation on a set of functions $\Psi_k(\boldsymbol{r}, \boldsymbol{R}(t))$, with coefficients $c_k(t)$, then the time evolution of the coefficients reads [12]:

$$i\frac{\partial c_k(t)}{\partial t} = \left[\hat{\mathcal{H}}_{kj}(\boldsymbol{r}, \boldsymbol{R}(t)) - i\left\langle \Psi_k \middle| \nabla_{\boldsymbol{R}} \middle| \Psi_j \right\rangle \cdot \frac{\mathrm{d}\boldsymbol{R}(t)}{\mathrm{d}t}\right] c_j(t). \tag{1.8}$$

The terms between brackets, the Hamiltonian matrix elements $\hat{\mathcal{H}}_{kj}$ and the second term that is the nonadiabatic coupling $\boldsymbol{d}_{kj}$ between states k and j, are responsible for transitions. Interestingly, $\hat{\mathcal{H}}_{kj}(\boldsymbol{r}, \boldsymbol{R}(t))$ and $\boldsymbol{d}_{kj}(\boldsymbol{r}, \boldsymbol{R}(t))$ do not explicitly depend on time in this representation. Their change is effectuated through the implicit time-dependence on the nuclear coordinates $\boldsymbol{R}(t)$. Therefore, finding the specific nuclear motion $\boldsymbol{R}'(t)$ that evolves the reactant state into the desired product state is key. This topic is covered in **Chapters 3,4,5** and **7** for photosynthetic and biomimetic systems.

To better understand the nature of $\boldsymbol{R}'(t)$ consider a subspace of the Hilbert space comprising two states as the only ones that can interact, against a background manifold of states that are energetically well separated. For illustrative purposes let these be an exciton $\Psi_e(\boldsymbol{r}, \boldsymbol{R}(t))$ and a charge transfer state $\Psi_c(\boldsymbol{r}, \boldsymbol{R}(t))$ with coefficients $c_e(t)$ and $c_c(t)$. A 2x2 density matrix $\Gamma(t)$ can then be constructed for these states as:

$$\Gamma(t) = \begin{bmatrix} a_{ee}(t) & a_{ec}(t) \\ a_{ce}(t) & a_{cc}(t) \end{bmatrix} = \begin{bmatrix} c_e(t)c_e(t)^* & c_e(t)c_c(t)^* \\ c_c(t)c_e(t)^* & c_c(t)c_c(t)^* \end{bmatrix}. \tag{1.9}$$

Here, the diagonal elements are the populations and the off-diagonal elements represent the coherences that mix the states [14]. Consider a nuclear motion $\boldsymbol{R}'(t)$ that oscillates at resonance with the matrix element $a_{ec}(t) = c_e(t)c_c(t)^*$ responsible for mixing the charge transfer into the exciton. The process of photoinduced charge transfer is most efficient when it couples to such coherent nuclear motion.

1.3 Natural Photosynthesis

1.3.1 The Bacterial Reaction Center

In bacterial photosynthesis all absorbed photons are converted into stable charge separated states by reaction center (bRC) complexes [15,16]. When a photon is absorbed by a light-active bacteriochlorophyll pigment the resulting electron-hole pair - the exciton - is neutral. Only when an electron is transferred to a neighbouring pigment and the resulting electron vacancy - the hole - is not, charges are separated. Given the identical nature of the pigments in photosynthesis and the invariable locus of the charge separation (the reaction center), the evolutionary optimization of solar energy transduction must be strongly linked to the protein matrix surrounding the pigments (Figure 1.5).

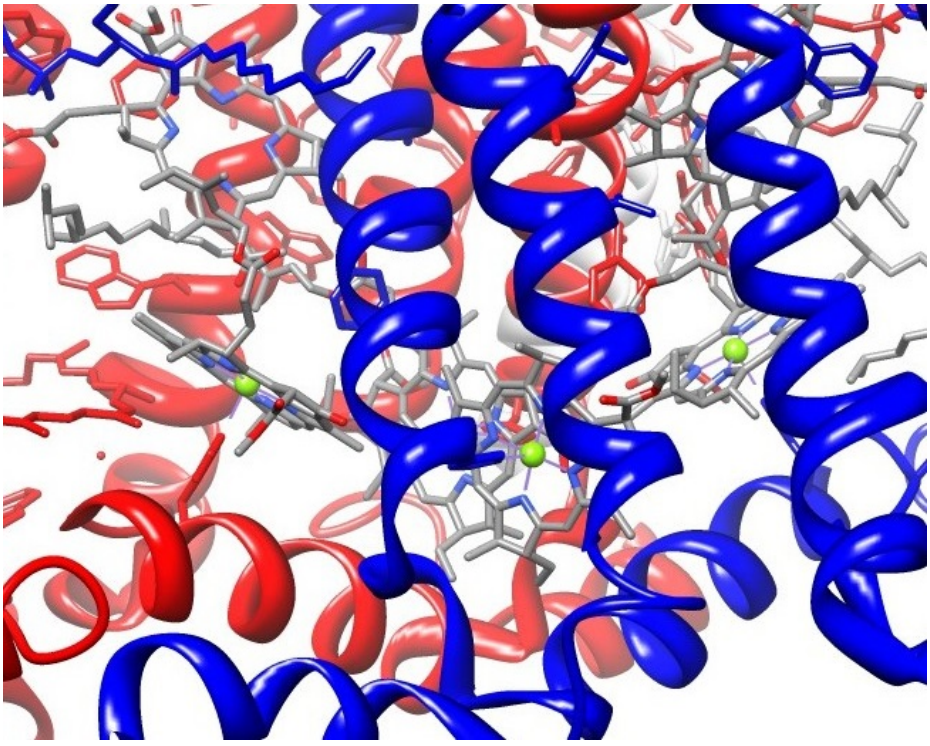

Figure 1.5: Zoomed-in view of the x-ray crystal structure of the *Rhodobacter Sphaeroides* reaction center (PDB-entry: 1M3X). The special pair bacteriochlorophylls (P) can be seen incased in the protein matrix, with on either side an accessory bacteriochlorophyll (B) and a bacteriopheophytin (H).

In fact, the vibrational spectrum of the site where excitons are dissociated in bRC - the special pair - differs markedly from that of its neighbouring pigment [17]. What is then the parameter that evolution has used to optimize charge separation? The answer may be specific coherent nuclear dynamics first reported in 1993 [18] that control the efficient evolution of excitons into separated charges ([19] and **Chapter 3** of this thesis). Figure 1.6 shows the pigments in bRC without the protein matrix. It can be seen that there is a two-fold symmetry between the cofactor branches. The special pair (P) is the closely coupled pair of bacteriochlorophylls (in white). Peripheral antenna complexes transfer photoinduced excitons to P. Here they are localized long enough to allow them to coherently couple to a low frequency collective mode of the pigments and the protein matrix (see **Chapter 3**). This mode introduces partial charge transfer character into the exciton (**Chapter 3**). The full charge separation takes place on a 3 ps timescale and involves a transfer of the excited electron to the accessory bacteriochlorophyll B_A ([20] and **Chapter 4**), while the hole remains on P. An interstitial water between P and B_A may play a crucial role in facilitating the full transfer ([21] and **Chapter 4**). Subsequent electron transfer from B_A to H_A (the right bottom red bacteriopheophytin in Figure 1.6) is fast and occurs on a 1 ps timescale.

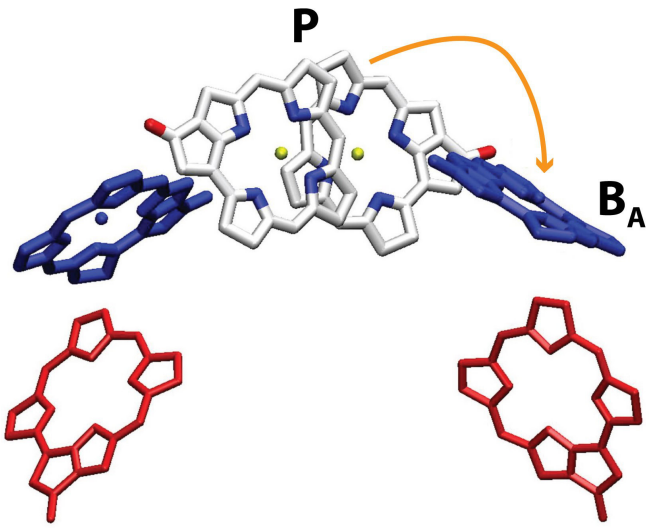

Figure 1.6: Twofold symmetric architecture of the bRC without protein environment. The first photoinduced electron transfer step (orange arrow) from P to B_A is illustrated.

1.3.2 Photosystem II

The Photosystem II reaction center (PSII) is commonly found in plants. It performs very efficient photoinduced charge separation and interfaces the charge separation with the slower process of water oxidation in the oxygen evolving center (OEC). Furthermore PSII posseses the highest known oxidation potential in living organisms (see **Chapter 6** of this thesis), which is required to drive the water oxidation. The branched structure of the chlorophyll pigments is shown in Figure 1.7 and comes from the latest highly accurate crystal structure [22].

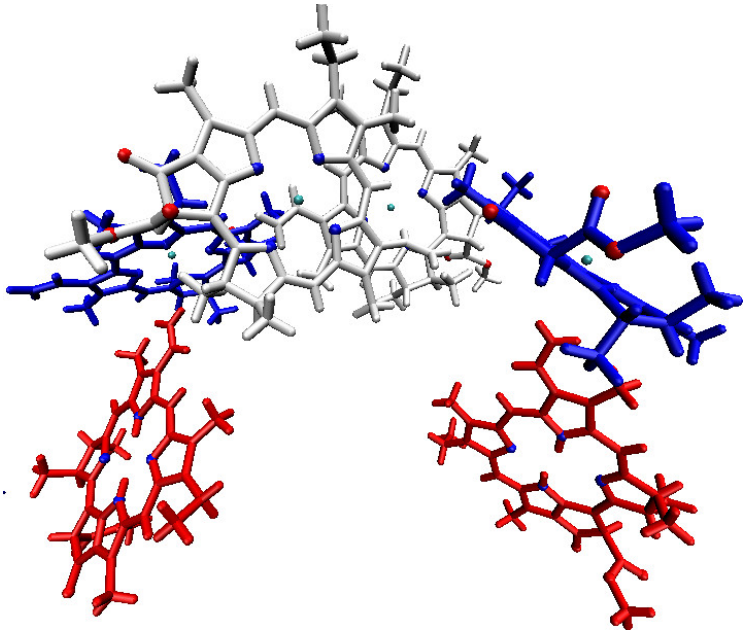

Figure 1.7: Twofold symmetric architecture of pigments in the Photosystem II reaction center without protein environment.

Interestingly the redox gradients between pigments in PSII are much smaller then in bRC (see [23] and **Chapter 6** of this thesis). To bridge the time scales of charge separation and catalysis an interstitial amino acid in the protein (Tyr_Z) is able to reversibly transfer a proton to another amino acid (His_Z) upon oxidation (see [24] and **Chapter 7** of this thesis). Finally, also in PSII very recently signatures of coherent nuclear motion coupled to photoinduced charge transfer have been observed [25,26] that drive the process along different charge separation pathways [27].

1.4 References

[1] Albert Einstein, Über einen die Erzeugung und Verwandlung des Lichtes betreffenden heuristischen Gesichtspunkt, *Annalen der Physik*, **1905**, 17, 132-148.

[2] Erwin Schrödinger, Quantisierung als Eigenwertproblem, *Annalen der Physik*, **1926**, (Erste Mitteilung) 79: 361-376, (Zweite Mitteilung) 79: 489-527, (Dreite Mitteilung) 80: 437-490, (Vierte Mitteilung) 81: 109-139.

[3] A. M. Dirac, (**1930**). The Principles of Quantum Mechanics.

[4] Michael Grätzel, Artificial photosynthesis: water cleavage into hydrogen and oxygen by visible light, *Accounts of Chemical Research*, **1981**, 14, 376-384.

[5] D. Gust, T. A. Moore, A. L. Moore. Solar fuels via artificial photosynthesis. *Accounts of chemical research*, **2009**, 42, 1890-898.

[6] B. O'Regan and M. Grätzel. A low-cost, high-efficiency solar cell based on dye-sensitized colloidal TiO_2 films, *Nature*, **1991**, 353, 737-740.

[7] N. S. Sariciftci, L. Smilowitz, A. J. Heeger, F. Wudl, Photoinduced Electron Transfer from a Conducting Polymer to Buckminsterfullerene, *Science*, **1992**, 258, 1474-1476.

[8] For example: http://gcell.com/ and http://www.heliatek.com/.

[9] J. D. Megiatto Jr, D. D. Mendez-Hernandez, M. E. Tejeda-Ferrari, A. Teillout, M. J. Llansola-Portoles, G. Kodis, O. G. Poluektov, T. Rajh, V. Mujica, T. L. Groy, D. Gust, T. A. Moore & A. L. Moore, A bioinspired redox relay that mimics radical interactions of the Tyr-His pairs of photosystem II, *Nature Chemistry*, **2014**, 6, 423-428.

[10] O. Khaselev and J. A. Turner, A Monolithic Photovoltaic-Photoelectrochemical Device for Hydrogen Production via Water Splitting, *Science*, **1998**, 280, 425-427.

[11] R. S. Mulliken and C. A. Rieke, Molecular electronic spectra, dispersion and polarization: The theoretical interpretation and computation of oscillator strengths and intensities, *Rep. Prog. Phys.*, **1941**, 8, 231.

[12] A. V. Akimov, A. J. Neukirch and O. V. Prezhdo, Theoretical Insights into Photoinduced Charge Transfer and Catalysis at Oxide Interfaces, *Chemical Reviews*, **2013**, 6, 4496.

[13] F. Buda, H. J. M. de Groot, A. Bifone, Charge localization and dynamics in rhodopsin, *Physical Review Letters*, 77, 4474-4477.

[14] C. Zener, Non-Adiabatic Crossing of Energy Levels. *Proceedings of the Royal Society A: Mathematical, Physical and Engineering Sciences*, **1932**, 137, 696-702.

[15] R. E. Blankenship, Molecular Mechanisms of Photosynthesis, **2014**, 2nd Ed. *Wiley-Blackwell*, Oxford, UK.

[16] Deisenhofer, J.; Epp, O.; Miki, K.; Huber, R.; Michel, H. Structure of the Protein Subunits in the Photosynthetic Reaction Centre of Rhodopseudomonas Viridis at 3Å Resolution. *Nature* **1985**, 318, 618-624.

[17] N. J. Cherepy, A. P. Shreve, L. J. Moore, S. Franzen, S. G. Boxer, R. A. Mathies, Near-Infrared Resonance Raman Spectroscopy of the Special Pair and the Accessory Bacteriochlorophylls in Photosynthetic Reaction Centers, *J. Phys. Chem.*, **1994**, 98, 602.

[18] M. H. Vos, F. Rappaport, J. C. Lambry, J. Breton, J. L. Martin, Visualization of coherent nuclear motion in a membrane protein by femtosecond spectroscopy, *Nature*, **1993**, 363, 320-325.

[19] Novoderezhkin, V.; Yakovlev, A.; van Grondelle, R.; Shuvalov, V. Coherent Nuclear and Electronic Dynamics in Primary Charge Separation in Photosynthetic Reaction Centers: A Redfield Theory Approach. *J. Phys. Chem. B*, **2004**, 108, 7445-7457.

[20] Holzapfel, W., Finkele, U., Kaiser, W., Oesterhelt, D., Scheer, H., Stilz, H.U., and Zinth, W., Initial electron-transfer in the reaction center from Rhodobacter sphaeroides, *PNAS* **1990**, 87, 5168-5172.

[21] Potter, J. A.; Fyfe, P. K.; Frolov, D.; Wakeham, M. C.; Grondelle, R. V.; Robert, B.; Jones, M. R. Strong Effects of an Individual Water Molecule on the Rate of Light-driven Charge Separation in the Rhodobacter sphaeroides Reaction Center. *Biochemistry* **2005**, 280, 27155-27164.

[22] Umena, Y., Kawakami, K., Shen, J.-R., and Kamiya, N., Crystal structure of oxygen-evolving photosystem II at a resolution of 1.9 Å, *Nature* **2011**, 473, 55-60.

[23] Konermann, L., and Holzwarth, A.R., Analysis of the absorption spectrum of photosystem II reaction centers: Temperature dependence, pigment assignment, and inhomogeneous broadening, *Biochemistry* **1996**, 35, 829-842.

[24] L. Hammarstom and S. Styring, Proton-coupled electron transfer of tyrosines in photosystem II and model systems for artificial photosynthesis, *Energy Environ. Sci.*, **2011**, 4, 2379-2388.

[25] Romero, E., Augulis, R., Novoderezhkin, V.I., Ferretti, M., Thieme, J., Zigmantas, D., and van Grondelle, R., Quantum coherence in photosynthesis for efficient solar-energy conversion, *Nature Physics* **2014**, *advanced publication*.

[26] Fuller, F.D., Pan, J., Gelzinis, A., Butkus, V., Senlik, S.S., Wilcox, D.E., Yocum, C.F., Valkunas, L., Abramavicius, D., and Ogilvie, J.P., Vibronic coherence in oxygenic photosynthesis, *Nature Chemistry* **2014**, 6, 706-711.

[27] Romero, E., van Stokkum, I.H.M., Novoderezhkin, V.I., Dekker, J.P., and van Grondelle, R, Two Different Charge Separation Pathways in Photosystem II, *Biochemistry* **2010**, 49, 4300-4307.